European Journal of Chemistry

View Journal Online
View Article Online

Synthesis, characterization, X-ray crystal structure and Hirshfeld surface analysis of Ni(II) complex of 1,2-bis(pyridin-2-ylmethylene)hydrazine

Meman Sahu [1], Amit Kumar Manna [1], Dinesh De [2] and Goutam Kumar Patra [1,*]

[1] *Department of Chemistry, Faculty of Physical Sciences, Guru Ghasidas Vishwavidyalaya, Bilaspur (Chhattisgarh), 495009, India*
[2] *Department of Basic Science, Vishwavidyalaya Engineering College, Ambikapur, CSVTU-Bhilai, Chhattisgarh, 497001, India*

* *Corresponding author at: Department of Chemistry, Faculty of Physical Sciences, Guru Ghasidas Vishwavidyalaya, Bilaspur (Chhattisgarh), 495009, India.*
e-mail: goutam.patra@ggu.ac.in (G.K. Patra).

RESEARCH ARTICLE

10.5155/eurjchem.13.1.1-7.2166

Received: 30 July 2021
Received in revised form: 05 September 2021
Accepted: 17 October 2021
Published online: 31 March 2022
Printed: 31 March 2022

KEYWORDS

Hydrazone
Ni(II)triple helix
Crystal structure
2-Pyridinaldazine
Hirshfeld surface analysis
1,2-Bis(Pyridin-2-ylmethylene)hydrazine

ABSTRACT

We report the synthesis, characterization, X-ray crystal structure and Hirshfeld surface analysis of Ni(II) perchlorate complex (1, $Ni_2L_3{\cdot}4ClO_4{\cdot}2CH_3CN$) of 1,2-*bis*(pyridin-2-ylmethylene)hydrazine (L) ligand. The X-ray crystallographic study of complex 1 reveals that in the presence of Ni(II) ions,the ligand L forms a dimeric triple helix with a Ni(II)-Ni(II) distance of 3.794 Å. Crystal data for $C_{40}H_{36}Cl_4N_{14}Ni_2O_{16}$: Monoclinic, space group $P2_1/c$ (no. 14), a = 20.7558(19) Å, b = 13.1937(12) Å, c = 20.0181(18) Å, β = 96.9510(10)°, V = 5441.6(9) Å^3, Z = 4, T = 293.15 K, μ(MoKα) = 0.965 mm^{-1}, D_{calc} = 1.498 g/cm^3, 38075 reflections measured (1.976° ≤ 2Θ ≤ 43.728°), 6557 unique (R_{int} = 0.0695, R_{sigma} = 0.0466) which were used in all calculations. The final R_1 was 0.0518 (I > 2σ(I)) and wR_2 was 0.1270 (all data). The Hirshfeld surface analysis of complex 1 shows that C···H, H···H, N···H and O···H interactions of 10.9, 26.4, 6.7, and 33.4%; respectively, which exposed that the main intermolecular interactions were H···H intermolecular interactions.

Cite this: *Eur. J. Chem.* **2022**, *13(1)*, 1-7 **Journal website**: www.eurjchem.com

1. Introduction

The simplest *bis*-pyridylimine ligand system is 1,2-*bis*(pyridin-2-ylmethylene)hydrazine (**L**) in which, two pyridin-2-ylmethanimine binding units are linked directly (no spacer) through the imine nitrogen atoms. **L** has the freedom to rotate about the central N-N bond. The coordination chemistry of **L** was first reported by Stratton and Busch in papers in 1958 and 1960 [1-3] and their studies are of specific historic importance to the field of metallo-supramolecular chemistry and in particular to helicate formation [4,5]. These scientists described the coordination of **L** with transition metal ions to form octahedral complexes with the formula $[M_2(L)_3]^{4+}$ (M = Co^{2+}, Fe^{2+} etc.) and documented that the species must comprise of three strands enfolded around two metals in a spiral fashion [6,7]. Their studies show the first recognized triple helicates. Helical complexes were exposed to exchange reactions on heating or standing to form mononuclear complexes $[M(L)_2]^{2+}$ in which the ligand twists to coordinate as a tridentate with a non-coordinated imine residue. Stratton and Busch proposed the term 'flexidentate' to describe the coordination behavior of ligand **L** [1-3]. Sheldrick *et al.* reported the X-ray crystal structure of the dinuclear triple-helical cobalt (II) complex formed from the pyridylmethyl ketazine ligand [8]. Hanon *et al.* first structurally characterized the dimeric Ag(I) triple helicate of **L** [9]. The relative positioning of the N atoms on the terminal pyridine ring and in the central part of the ligand **L** can easily be modified as needed in the design [10]. The ligand **L** can chelate any metal ion due to the close proximity of the pyridine ring N atom and the imine N atom of the body of the ligand [11].

Aggravated by the above facts and in continuation of our ongoing research work in search for metal complexes of imino-pyridyl ligands of potential importance [12-18], we have reported here the synthesis, crystal structure and Hirshfeld surface analysis of the nickel(II) complex of 1,2-*bis*(pyridin-2-ylmethylene)hydrazine.

2. Experimental

2.1. Materials and physical measurements

All chemicals used in this study were purchased from Aldrich Chemical Company, USA, and Acros Chemical Company, USA, and used without further purification unless otherwise mentioned. The melting point was determined by an electro-thermal IA9000 series digital melting point apparatus and is uncorrected. Microanalyses were performed using a Perkin Elmer 2400II elemental analyzer.

ISSN 2153-2249 (Print) / ISSN 2153-2257 (Online)

https://dx.doi.org/10.5155/eurjchem.13.1.1-7.2166

Table 1. Crystal data and structure refinement for complex **1**.

Empirical formula	$C_{40}H_{35}Cl_4N_{14}Ni_2O_{16}$
Formula weight	1227.04
Temperature (K)	293.15
Crystal System	Monoclinic
Space group	$P2_1/c$
a, (Å)	20.7558(19)
b, (Å)	13.1937(12)
c, (Å)	20.0181(18)
α (°)	90
β (°)	96.9510(10)
γ (°)	90
Volume (Å^3)	5441.6(9)
Z	4
ρ_{calc}(g/cm^3)	1.498
μ (mm^{-1})	0.965
F(000)	2500.0
Crystal size (mm^3)	0.18 × 0.16 × 0.12
Radiation	MoKα (λ = 0.71073)
2Θ range for data collection (°)	1.976 to 43.728
Index ranges	$-21 \leq h \leq 21$, $-13 \leq k \leq 13$, $-20 \leq l \leq 20$
Reflections collected	38075
Independent reflections	6557 [R_{int} = 0.0695, R_{sigma} = 0.0466]
Data/restraints/parameters	6557/0/724
Goodness-of-fit on F^2	1.050
Final R indexes [I≥2σ (I)]	R_1 = 0.0518, wR_2 = 0.1192
Final R indexes [all data]	R_1 = 0.0675, wR_2 = 0.1270
Largest diff. peak/hole (e.Å^{-3})	0.90/-0.75

Infrared (IR) and solution electronic spectra were recorded on Nicolet Magna IR (Series II) and Shimadzu UV-160A spectrophotometers, respectively. ESI-mass spectra were recorded on a Waters mass spectrometer using mixed solvent methanol and triple distilled water.

2.2. Synthesis of the ligand,1,2-bis(pyridin-2-ylmethylene) hydrazine (L)

The ligand **L** was prepared by refluxing 2-pyridine-carboxaldehyde and hydrazine hydrate in 2:1 molar ratio in methanol, following the reported procedure [1,3].

1,2-*Bis*(Pyridin-2-ylmethylene)hydrazine (**L**): Color: Yellow. Yield: 85%. M.p.: 113-115 °C. ESI-MS (*m/z*, %): 211.23 (L$^+$, 100%). Anal. calcd. for $C_{12}H_{10}N_4$: C, 68.56; H, 4.79; N, 26.65. Found: C, 68.78.; H, 4.67; N, 26.44%. FT-IR (KBr, ν, cm^{-1}): 2925 (wb, Aromatic C-H), 1628 (vs, C=N), 1485 (s, N-N), 1043 (m, Aliphatic C-H). UV-Vis (CH_3OH, λ, nm (ε, M^{-1}cm^{-1})): 210 (8200), 237 (13800), 275 (9400).

2.3. Synthesis of nickel(II) perchlorate complex (1)

To 20 mL yellowish methanol solution of **L** (0.158 g, 0.75 mmol) was added solid $Ni(ClO_4)_2.6H_2O$ (0.185 g, 0.50 mmol). The reaction mixture was stirred for 3 h. The brown precipitate obtained was filtered off and dried in air. It was then dissolved in acetonitrile and kept in the refrigerator overnight. Reddish brown crystalline complexes suitable for X-ray single crystal diffraction analysis were obtained, filtered off, washed with 5 mL of methanol, and dried in vacuum over fused $CaCl_2$. The single crystals of complex **1** were obtained by the direct diffusion of diethyl ether in the acetonitrile solution of **L**.

Complex **1**: Color: Reddish brown. Yield: 75%. M.p.: 200-201 °C. FT-IR (KBr, ν, cm^{-1}): 3437 (wb), 3043 (w), 2947 (m), 2856 (m), 2015 (w) 1645 (s), 1615 (s), 1458 (w), 1412 (m), 1318 (w), 1245 (m), 1107 (s), 825 (s), 629 (s).

CAUTION! Although while working with the perchlorate complex described here, we have not met with any incident, care should be taken in handling them, as perchlorates are potentially explosive. They should not be prepared and stored in large amounts.

2.4. X-ray crystallography

Single crystal X-ray data of complex **1** was collected using MoKα (λ = 0.71073 Å) radiation on a Bruker APEX II diffractometer equipped with CCD area detector. The crystal was kept at 293.15 K during data collection. Using Olex2 [19], the structure was solved with the SHELXS [20] structure solution program using Direct Methods and refined with the SHELXL [21] refinement package using Least Squares minimisation. Atoms other than hydrogen atoms were treated anisotropically. The hydrogen atoms were geometrically fixed. The crystallographic details of complex **1** are summarized in Table 1, the selected bond lengths and angles of complex **1** are also listed in Tables 2 and 3.

2.5. Hirshfeld surface calculations

For obtaining additional insight into the intermolecular interaction of molecular crystals, Hirshfeld surface analysis helps as a powerful set-up. The size and shape of Hirshfeld surface allow the qualitative and quantitative study and imagining of intermolecular close contacts in molecular crystals [22]. Molecular Hirshfeld surfaces are built based on electron distribution calculated as the sum of spherical atom electron densities [23,24]. Thus, an isosurface is obtained, and for each point of the isosurface, two distances can be defined: d_e, the distance from the point to the nearest atom outside to the surface, and d_i, the distance to the nearest atom inside to the surface. Furthermore, the identification of the regions of particular importance for intermolecular interactions is achieved by mapping the normalized contact distance (d_{norm}), expressed as: $d_{norm} = (d_i - r_i^{vdw})/r_i^{vdw} + (d_e - r_e^{vdw})/r_e^{vdw}$; where r_i^{vdw} and r_e^{vdw} are the van der Waals radii of the atoms [25]. The value of d_{norm} is negative or positive when intermolecular contacts are shorter than or longer than r^{vdw}, respectively.

Table 2. Selected bond lengths for complex **1**.

Atom	Atom	Length (Å)	Atom	Atom	Length (Å)	Atom	Atom	Length (Å)
Ni1	N3	2.084(4)	C11	C12	1.465(8)	C23	C22	1.386(8)
Ni1	N4	2.090(4)	C8	C7	1.380(8)	C23	N7	1.340(7)
Ni1	N5	2.085(4)	C8	C9	1.364(8)	C21	C22	1.381(8)
Ni1	N11	2.084(4)	C7	N3	1.336(7)	N8	C24	1.094(11)
Ni1	N12	2.086(4)	C9	C10	1.395(8)	C24	C25	1.465(13)
Ni1	N13	2.090(4)	N4	C12	1.272(6)	N9	C26	1.364(7)
Ni2	N1	2.085(4)	N4	N10	1.400(6)	N9	C30	1.338(7)
Ni2	N2	2.080(4)	C16	C17	1.384(7)	C26	C27	1.378(7)
Ni2	N6	2.078(4)	C16	C15	1.385(8)	C26	C31	1.467(7)
Ni2	N7	2.074(4)	C37	C36	1.372(8)	C27	C28	1.386(8)
Ni2	N9	2.076(4)	C17	N5	1.347(7)	C30	C29	1.391(8)
Ni2	N10	2.083(4)	C17	C32	1.456(7)	C28	C29	1.373(8)
C1	C2	1.375(7)	C14	C13	1.387(8)	N10	C31	1.277(7)
C1	N1	1.354(7)	C14	C15	1.357(8)	C32	N11	1.273(6)
C1	C6	1.466(7)	C13	N5	1.345(7)	N12	C34	1.360(7)
C2	C3	1.394(8)	N6	C50	1.272(6)	N12	C35	1.332(7)
C3	C4	1.354(8)	N6	N11	1.403(6)	N13	C33	1.277(6)
C4	C5	1.392(8)	C19	C20	1.380(8)	C34	C33	1.481(7)
C5	N1	1.338(7)	C19	C50	1.462(7)	C34	C38	1.379(7)
N2	C6	1.273(6)	C19	N7	1.350(7)	C35	C36	1.390(8)
N2	N13	1.401(6)	C20	C21	1.375(8)	C38	C37	1.386(8)
C11	C10	1.378(8)	C11	N3	1.357(7)	N15	C42	1.092(8)

Table 3. Bond angles for complex **1**.

Atom	Atom	Atom	Angle (°)	Atom	Atom	Atom	Angle (°)	Atom	Atom	Atom	Angle (°)
N3	Ni1	N4	76.97(17)	C5	N1	Ni2	127.3(4)	C21	C20	C19	119.0(5)
N3	Ni1	N5	95.46(17)	C5	N1	C1	118.3(5)	N7	C23	C22	122.2(6)
N3	Ni1	N11	100.69(16)	C6	N2	Ni2	117.0(4)	C20	C21	C22	119.1(6)
N3	Ni1	N12	96.62(16)	C6	N2	N13	121.0(4)	N6	C50	C19	115.5(5)
N3	Ni1	N13	163.05(17)	N13	N2	Ni2	121.0(3)	C21	C22	C23	119.1(6)
N4	Ni1	N13	88.51(16)	N2	C6	C1	116.2(5)	C19	N7	Ni2	114.4(3)
N5	Ni1	N4	161.85(17)	C10	C11	C12	122.7(5)	C23	N7	Ni2	127.1(4)
N5	Ni1	N12	96.88(17)	N3	C11	C10	123.0(5)	C23	N7	C19	118.2(5)
N5	Ni1	N13	100.91(16)	N3	C11	C12	114.3(5)	N8	C24	C25	169.7(14)
N11	Ni1	N4	88.00(17)	C9	C8	C7	119.3(6)	C26	N9	Ni2	114.3(3)
N11	Ni1	N5	77.10(17)	N3	C7	C8	123.4(6)	C30	N9	Ni2	128.4(4)
N11	Ni1	N12	162.11(17)	C8	C9	C10	118.8(5)	C30	N9	C26	117.2(5)
N11	Ni1	N13	87.30(16)	C11	C10	C9	118.5(6)	N9	C26	C27	122.9(5)
N12	Ni1	N4	100.35(16)	C11	N3	Ni1	114.8(3)	N9	C26	C31	115.1(5)
N12	Ni1	N13	77.22(16)	C7	N3	Ni1	128.3(4)	C27	C26	C31	121.9(5)
N2	Ni2	N1	77.34(17)	C7	N3	C11	116.9(5)	C26	C27	C28	119.0(6)
N2	Ni2	N10	88.17(17)	C12	N4	Ni1	116.2(4)	N9	C30	C29	122.5(6)
N6	Ni2	N1	99.72(16)	N15	C42	C43	178.2(9)	C29	C28	C27	118.5(5)
N6	Ni2	N2	87.78(16)	N12	C35	C36	123.3(5)	C28	C29	C30	119.8(6)
N6	Ni2	N10	89.18(17)	C12	N4	N10	120.2(4)	N4	N10	Ni2	120.6(3)
N7	Ni2	N1	94.86(17)	N10	N4	Ni1	120.6(3)	C31	N10	Ni2	117.0(4)
N7	Ni2	N2	161.72(17)	N4	C12	C11	116.3(5)	C31	N10	N4	119.3(5)
N7	Ni2	N6	77.17(17)	C17	C16	C15	119.0(5)	N10	C31	C26	115.5(5)
N7	Ni2	N9	99.00(17)	C16	C17	C32	122.0(5)	N11	C32	C17	116.4(5)
N7	Ni2	N10	101.74(17)	N5	C17	C16	122.9(5)	N6	N11	Ni1	121.6(3)
N9	Ni2	N1	95.01(17)	N5	C17	C32	115.1(5)	C32	N11	Ni1	116.7(4)
N9	Ni2	N2	98.13(16)	C15	C14	C13	119.5(5)	C32	N11	N6	120.4(4)
N9	Ni2	N6	165.02(17)	N5	C13	C14	122.9(5)	C34	N12	Ni1	114.3(3)
N9	Ni2	N10	77.33(18)	C14	C15	C16	118.8(5)	C35	N12	Ni1	128.6(4)
N10	Ni2	N1	162.58(17)	C17	N5	Ni1	114.5(3)	C35	N12	C34	117.0(4)
C2	C1	C6	122.1(5)	C13	N5	Ni1	128.6(4)	N2	N13	Ni1	121.4(3)
N1	C1	C2	122.9(5)	C13	N5	C17	116.9(5)	C33	N13	Ni1	117.9(3)
N1	C1	C6	114.9(5)	C50	N6	Ni2	117.3(4)	C33	N13	N2	119.7(4)
C1	C2	C3	118.1(6)	C50	N6	N11	120.9(4)	N12	C34	C33	115.4(5)
C4	C3	C2	119.1(6)	N11	N6	Ni2	121.0(3)	N12	C34	C38	123.4(5)
C3	C4	C5	120.3(6)	C20	C19	C50	122.3(5)	C38	C34	C33	121.1(5)
N1	C5	C4	121.2(6)	N7	C19	C20	122.5(5)	N13	C33	C34	114.9(5)
C1	N1	Ni2	114.3(3)	N7	C19	C50	115.2(5)	C34	C38	C37	118.0(5)

The graphical plots of the molecular Hirshfeld surfaces mapped with d_{norm} employ the red-white-blue color scheme, where the red color indicates the shorter intermolecular contacts, white color shows the contacts around the r^{vdw} separation, and blue color is used to point out the longer contact distances. Due to the symmetry between d_e and d_i in the expression for d_{norm}, where two Hirshfeld surfaces touch, both will display a red spot identical in color intensity as well as size and shape [26]. The mixture of d_e and d_i in the form of a 2D fingerprint plot provides a summary of intermolecular contacts in the crystal and are in complement to the Hirshfeld surfaces [22]. The information about the intermolecular interactions in the immediate environment of each molecule in the asymmetric unit is achieved by such plots. In addition, the close contacts between particular atom types can be highlighted in so-called resolved fingerprint plots [27], which allow the facile assignment of an intermolecular contact to a certain type of interaction and quantitatively summarize the nature and type of intermolecular contacts. Two additional colored properties (shape index and curvedness) based on the local curvature of the surface can also be specified [28]. The Hirshfeld surfaces are mapped with d_{norm}, shape-index, curvedness and 2D fingerprint plots (full and resolved) reported in this manuscript were generated using Crystal-Explorer 3.1 [29].

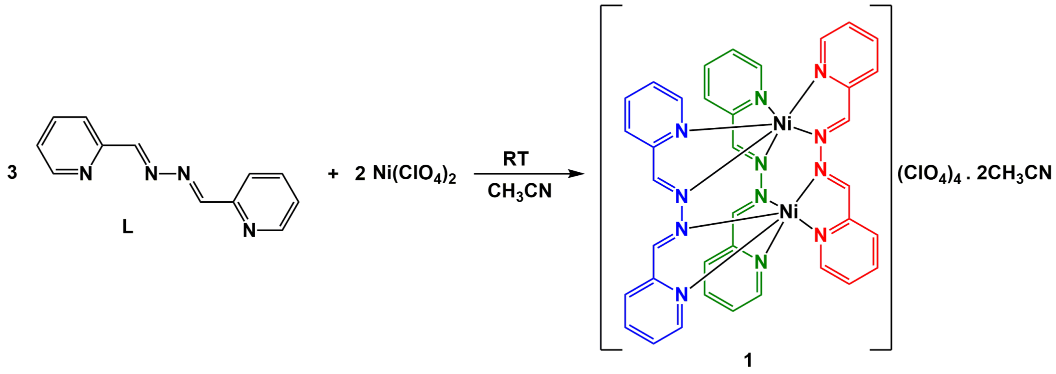

Scheme 1. Synthesis of complex **1**.

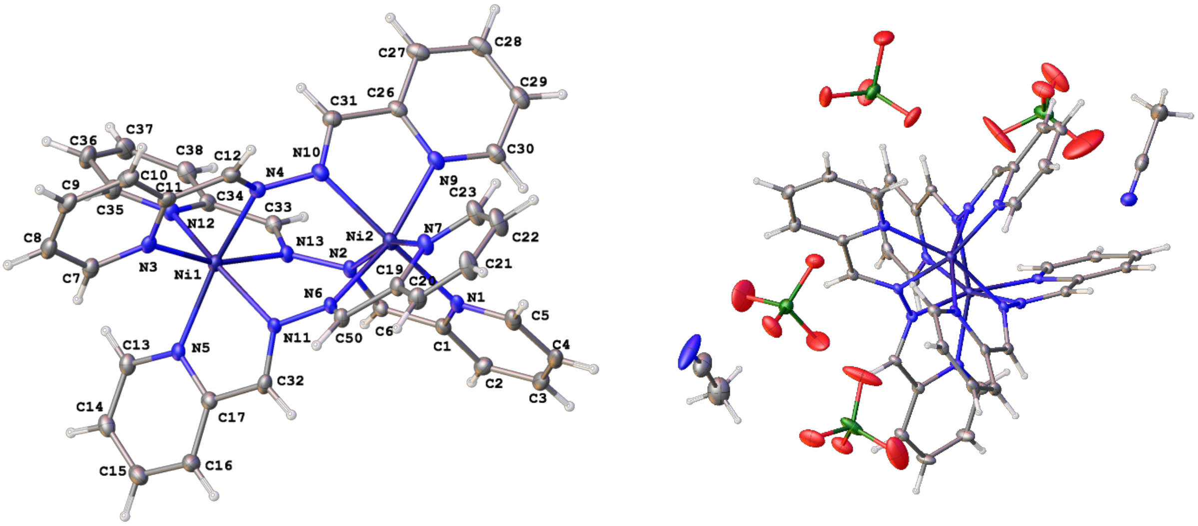

Figure 1. The molecular structure of complex **1**.

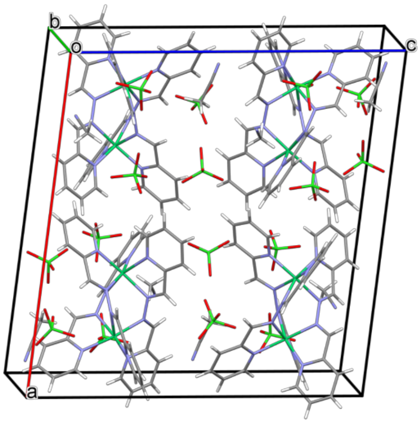

Figure 2. The packing diagram of complex **1**.

3. Results and discussion

3.1. Synthetic aspects

The ligand **L** is 2 + 1 condensates of 2-pyridinecarbaldehyde and hydrazine (Scheme 1). The reddish brown Ni(II) perchlorate complex (**1**) has been synthesized in good yield by reacting $Ni(ClO_4)_2$ with the ligand **L** at room temperature in a 2:3 molar proportion. Complex **1** has been characterized by elemental analysis and IR spectra as well as by single crystal X-ray diffraction studies.

3.2. Structural description of complex 1

The Ni(II) complex of **L** crystallizes with two molecules of acetonitrile. The X-ray crystallographic study of complex **1** reveals that in the presence of Ni(II) ions the ligand gives rise to a dimeric triple helix (Figure 1). The packing diagram of complex **1** has been presented in Figure 2. Each Ni(II) center binds to three ligand strands thereby attaining a pseudo-octahedral coordination geometry. The two Ni(II) centers are separated by a distance of 3.794 Å.

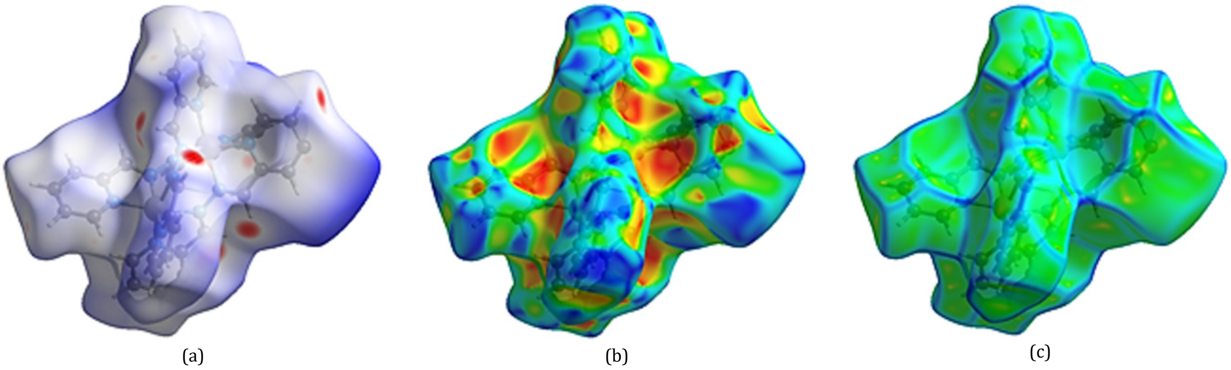
(a) (b) (c)

Figure 3. Hirshfeld surfaces of complex **1**, (a) 3D d_{norm} surface, (b) shape index and (c) curvedness.

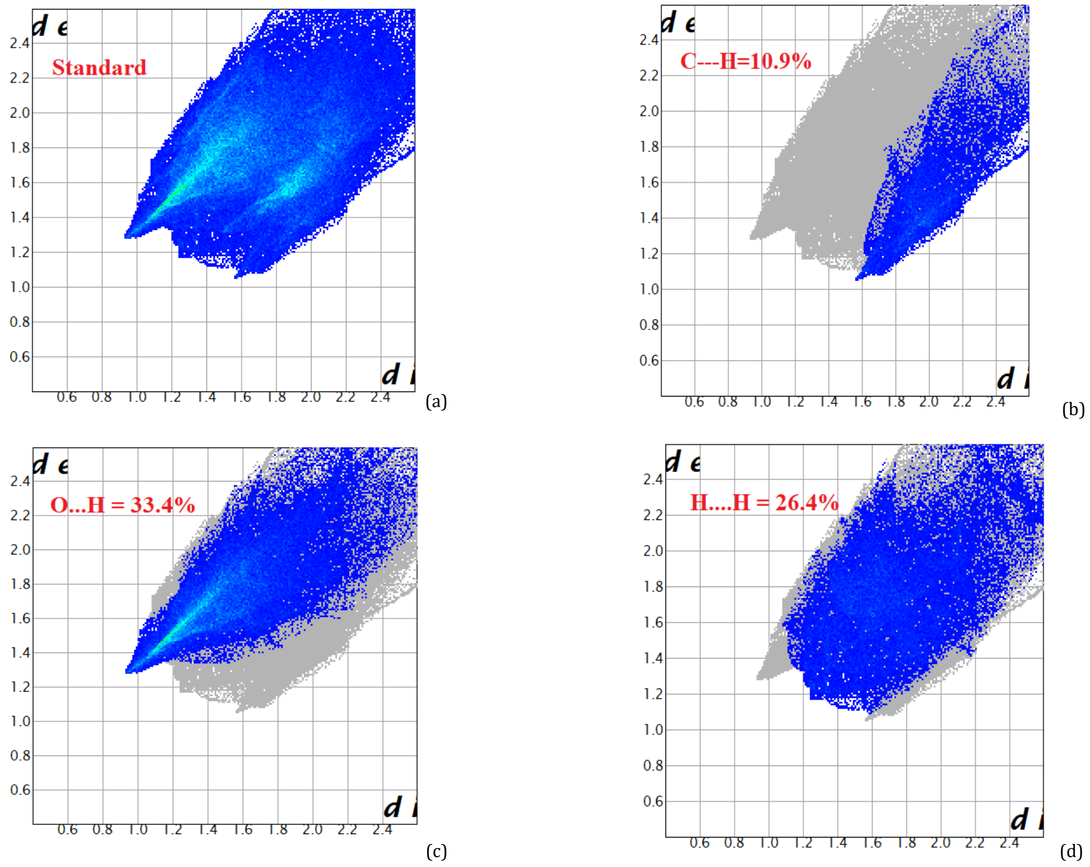

Figure 4. 2D fingerprint plots of complex **1**, (a) standard full, (b) resolved into C···H, (c) resolved into O···H and (d) H···H contacts, showing the percentages of contacts that contribute to the total Hirshfeld surface area of the molecule.

The bond lengths to the imine groups (mean 2.086 Å) are slightly longer than those to the pyridine units (mean 2.083 Å). This may be a consequence of the helical structure, but could also imply more effective σ-donation or π-back donation. The imine units are fundamentally planar and the helical twist is achieved primarily by twisting about the central N–N bond. There are no significant π-π interactions between the pyridine rings either within or without the helicates. However, other supramolecular interactions are present in the structure. Consistent with this, two molecules of the acetonitrile solvent per helical cation are incorporated into the crystal lattice, and these solvent molecules appear to play an important role in the supra-molecular stabilization of the acidic imine-CH protons. Amongst the four perchlorate anions, two are disordered.

3.3. Theoretical investigations

The Hirshfeld surface is a suitable tool for describing the surface characteristics of molecules. The molecular Hirshfeld surface of complex **1** was generated using a standard (high) surface resolution with the 3D d_{norm} surfaces mapped over a fixed color scale of -0.22 (red) to 1.4 Å (blue). The shape index mapped in the color range of -0.99 to 1.0, and Curvedness was in the range of -4.0 to 0.4. The surfaces were shown to be transparent to allow visualization of the molecular moiety in a similar orientation for all of the structures around which they were calculated. The molecular Hirshfeld surface (d_{norm}, Shape index and Curvedness) of complex **1** has been shown in Figure 3.

The dispositions adopted by the molecules in the crystal packing lead to close contact that could be quantified by the mapping of the two-dimensional fingerprint. The fingerprint plot indicates the contributions of interatomic contacts to the Hirshfeld surfaces of the crystal packing. The Hirshfeld surface analysis of complex **1** shows that C···H, O···H, and H···H interactions of 10.9, 33.4, and 26.4%, respectively, from which it is clear that the main intermolecular interactions are O···H intermolecular interactions. Both the C···H and N···H interactions were represented almost same area by a small area in the right side of the top in the 2D fingerprint map, whereas the O···H interactions were represented by the largest in the fingerprint plot (Figure 4) and thus had the most significant contribution to the total Hirshfeld surfaces (33.4 %).

4. Conclusion

Herein, the shortest *bis* Schiff base imino-pyridyl ligand **L** and its Ni(II) perchlorate complex **1** have been reported. The detailed X-ray single crystal structure and theoretical studies of complex **1** have also been performed. Complex **1** represents a dinuclear triple helix of **L**. A pseudo-octahedral geometry has been observed in the X-ray single crystal structure of complex **1**. The Hirshfeld surface analysis of the complex **1** shows that C···H, O···H, and H···H interactions of 10.9, 33.4, and 26.4%, respectively.

Acknowledgements

Goutam Kumar Patra would like to thank the Department of Science and Technology (SR/FST/CSI-264/2014 and EMR/2017/0001789) and the Department of Biotechnology, Government of India, New Delhi for financial support. Meman Sahu thanks the Council for Scientific and Industrial Research, Government of India, for financial support in the form of research fellowships.

Supporting information

CCDC-807524 contains the supplementary crystallographic data for this paper. These data can be obtained free of charge via https://www.ccdc.cam.ac.uk/structures/, or by e-mailing data_request@ccdc.cam.ac.uk, or by contacting The Cambridge Crystallographic Data Centre, 12 Union Road, Cambridge CB2 1EZ, UK; fax: +44(0)1223-336033.

Disclosure statement

Conflict of interest: The authors declare that they have no conflict of interest.
Ethical approval: All ethical guidelines have been adhered.
Sample availability: Samples of the compounds are available from the author.

CRediT authorship contribution statement

Conceptualization: Goutam Kumar Patra; Methodology: Amit Kumar Manna; Software: Dinesh De; Validation: Meman Sahu; Formal Analysis: Meman Sahu; Investigation: Meman Sahu; Resources: Goutam Kumar Patra; Data Curation: Dinesh De; Writing - Original Draft: Goutam Kumar Patra; Writing - Review and Editing: Goutam Kumar Patra; Visualization: Goutam Kumar Patra; Funding acquisition: Goutam Kumar Patra; Supervision: Goutam Kumar Patra; Project Administration: Goutam Kumar Patra.

ORCID and Email

Meman Sahu
memansahu8@gmail.com
https://orcid.org/0000-0001-9397-4805
Amit Kumar Manna
amitmanna51@gmail.com
https://orcid.org/0000-0002-9605-2168
Dinesh De
d2chem@gmail.com
https://orcid.org/0000-0001-7850-8718
Goutam Kumar Patra
goutam.patra@ggu.ac.in
https://orcid.org/0000-0003-3151-0284

References

[1]. Stratton, W. J.; Busch, D. H. The Complexes of Pyridinaldazine with Iron(II) and Nickel(II). *J. Am. Chem. Soc.* **1958**, *80* (6), 1286–1289.

[2]. Stratton, W. J.; Busch, D. H. The Complexes of Pyridinaldazine with Iron(II) and Nickel(II). II. *J. Am. Chem. Soc.* **1958**, *80* (13), 3191–3195.

[3]. Stratton, W. J.; Busch, D. H. The Complexes of Pyridinaldazine. III. Infrared Spectra and Continued Synthetic Studies. *J. Am. Chem. Soc.* **1960**, *82* (18), 4834–4839.

[4]. Zimmer, M.; Tocher, D. A.; Patra, G. K.; Naskar, J. P.; Datta, D. First Example of a Double Stranded Helicate with Square-Planar Coordination for the Metal. *Indian J. Chem. Sect. A* **1999**, *38*, 1087–1091.

[5]. Pal, P. K.; Chowdhury, S.; Purkayastha, P.; Tocher, D. A.; Datta, D. A Novel Double-Stranded Dinuclear Copper(I) Helicate Having a Photoluminescent CuI2N8 Chromophore. *Inorg. Chem. Commun.* **2000**, *3* (11), 585–589.

[6]. Stratton, W. J. Metal Complexes with Azine Ligands. II. Iron(II), Cobalt(II), and Nickel(II) Complexes with 2-Pyridyl Methyl Ketazine. *Inorg. Chem.* **1970**, *9* (3), 517–520.

[7]. Stratton, W. J.; Rettig, M. F.; Drury, R. F. Metal Complexes with Azine Ligands. I. Ligand Hydrolysis and Template Synthesis in the Iron(II)-2-Pyridinaldazine System. *Inorganica Chim. Acta* **1969**, *3*, 97–102.

[8]. Boyd, P. D. W.; Gerloch, M.; Sheldrick, G. M. Crystal Structure of Tris-μ-[2,5-Di(2-Pyridyl)-3,4-Diazahexa-2,4-Diene]-Dicobalt(II) Di[Aquotrichlorozincate(II)] Tetrachlorozincate(II) Tetrahydrate: A Helical Binuclear Cobalt(II) Cation. *J. Chem. Soc., Dalton Trans.* **1974**, No. 10, 1097–1102.

[9]. Hamblin, J.; Jackson, A.; Alcock, N. W.; Hannon, M. J. Triple Helicates and Planar Dimers Arising from Silver(i) Coordination to Directly Linked Bis-Pyridylimine Ligands. *J. Chem. Soc.* **2002**, No. 8, 1635.

[10]. Pal, S.; Pal, S. Syntheses, Structures and Properties of Trans-Dichloro ruthenium(II) Complexes with N4-Donor Schiff Bases. *Polyhedron* **2003**, *22* (6), 867–873.

[11]. Mukherjee, A.; Dutta, A.; Jana, A. D.; Patra, G. K. Copper(I) and Silver(I) Coordination Assemblies of Imino-Pyridyl and Azino-Pyridyl Ligands: Syntheses, Crystal Structures, Spectroscopic and Photophysical Properties. *Inorganica Chim. Acta* **2013**, *404*, 131–143.

[12]. Mukherjee, A.; Chakrabarty, R.; Ng, S. W.; Patra, G. K. The Syntheses, Characterizations, X-Ray Crystal Structures and Properties of Cu(I) Complexes of a Bis-Bidentate Schiff Base Ligand. *Inorganica Chim. Acta* **2010**, *363* (8), 1707–1712.

[13]. Patra, G. K.; Pal, P. K.; Mondal, J.; Ghorai, A.; Mukherjee, A.; Saha, R.; Fun, H.-K. Predesigned Synthesis of Dinuclear to Unusual Hexanuclear to 1D Coordination Polymer of Cu(I)-Halides and Their Photophysical Properties. *Inorganica Chim. Acta* **2016**, *447*, 77–86.

[14]. Mondal, J.; Mukherjee, A.; Patra, G. K. CuX (X = I, Br and Cl) Based Coordination Polymers of Azino-Pyridyl Ligand and PPh3: Structural, Spectral, Electro-Chemical, and DFT Studies. *Inorganica Chim. Acta* **2017**, *463*, 44–53.

[15]. Manna, A. K.; Mondal, J.; Chandra, R.; Rout, K.; Patra, G. K. A Thio-Urea Based Chromogenic and Fluorogenic Chemosensor for Expeditious Detection of Cu2+, Hg2+ and Ag+ Ions in Aqueous Medium. *J. Photochem. Photobiol. A Chem.* **2018**, *356*, 477–488.

[16]. Patra, G. K.; Goldberg, I.; Chowdhury, S. K.; Maiti, B. C.; Sarkar, A.; Bangal, P. R.; Chakravorti, S.; Chattopadhyay, N.; Tocher, D. A.; Drew, M. G. B.; Mostafa, G.; Chowdhury, S.; Datta, D. A New Photoluminescent CuI2N6 Chromophore. *New J. Chem.* **2001**, *25* (11), 1371–1373.

[17]. Patra, G. K.; Goldberg, I.; De, S.; Datta, D. Effect of the Size of Discrete Anions on the Nuclearity of a Complex Cation. *CrystEngComm* **2007**, *9* (9), 828–832.

[18]. Patra, G. K.; Goldberg, I. Syntheses and Crystal Structures of Copper and Silver Complexes with New Imine Ligands – Air-Stable, Photoluminescent CuIN4 Chromophores. *Eur. J. Inorg. Chem.* **2003**, *2003* (5), 969–977.

[19]. Dolomanov, O. V.; Bourhis, L. J.; Gildea, R. J; Howard, J. A. K.; Puschmann, H. OLEX2: a complete structure solution, refinement and analysis program. *J. Appl. Cryst.* **2009**, *42*, 339–341.

[20]. Sheldrick, G. M. A short history of SHELX. *Acta Crystallogr. A* **2008**, *64*, 112–122.

[21]. Sheldrick, G. M. Crystal structure refinement with SHELX. *Acta Crystallogr. C Struct. Chem.* **2015**, *71*, 3–8.

[22]. Norret, M.; Makha, M.; Sobolev, A. N.; Raston, C. L. Controlling the Confinement of Fullerene C60 Molecules Using a Saddle Shape Ni(Ii) Macrocycle. *New J. Chem.* **2008**, *32* (5), 808–812.

[23]. Spackman, M. A.; McKinnon, J. J. Fingerprinting Intermolecular Interactions in Molecular Crystals. *CrystEngComm* **2002**, *4* (66), 378–392.

[24]. Meng, X. X. Applications of Hirshfeld surfaces to ionic and mineral crystals, Ph.D. Thesis, University of New England, 2004.

[25]. Pendás, A. M.; Luaña, V.; Pueyo, L.; Francisco, E.; Mori-Sánchez, P. Hirshfeld Surfaces as Approximations to Interatomic Surfaces. *J. Chem. Phys.* **2002**, *117* (3), 1017–1023.

[26]. Desiraju, G. R. Crystal Engineering: A Holistic View. *Angew. Chem. Int. Ed. Engl.* **2007**, *46* (44), 8342–8356.

[27]. McKinnon, J. J.; Fabbiani, F. P. A.; Spackman, M. A. Comparison of Polymorphic Molecular Crystal Structures through Hirshfeld Surface Analysis. *Cryst. Growth Des.* **2007**, *7* (4), 755–769.

[28]. Schmidt, G. M. J. Photodimerization in the Solid State. *Pure Appl. Chem.* **1971**, *27* (4), 647–678.

[29]. Wolff, S. K.; Grimwood, D. J.; McKinnon, J. J.; Turner, M. J.; Jayatilaka, D.; Spackman, M. A. CrystalExplorer (Version 3.1), University of Western Australia, 2012.